Steel and Composite Structures, *Vol. 22, No. 4 (2016) 915-935*
DOI: http://dx.doi.org/10.12989/scs.2016.22.4.915

Nonlinear behavior of connections in RCS frames with bracing and steel plate shear wall

Saeedeh Ghods [1], Ali Kheyroddin [*1], Meissam Nazeryan [2], Seyed Masoud Mirtaheri [3] and Majid Gholhaki [1]

[1] *Depatment of Civil Engineering, Semnan University, Semnan, Iran*
[2] *Depatment of Civil engineering, Sharif University of Technology, Tehran, Iran*
[3] *Department of Civil Engineering, K.N. Toosi University of Technology, Tehran, Iran*

(*Received June 26, 2016, Revised October 24, 2016, Accepted November 11, 2016*)

Abstract. Steel systems composed of Reinforced Concrete column to Steel beam connection (RCS) have been raised as a structural system in the past few years. The optimized combination of steel-concrete structural elements has the advantages of both systems. Through beam and through column connections are two main categories in RCS systems. This study includes finite-element analyses of mentioned connection to investigate the seismic performance of RCS connections. The finite element model using ABAQUS software has been verified with experimental results of a through beam type connection tested in Taiwan in 2005. According to verified finite element model a parametric study has been carried out on five RCS frames with different types of lateral restraint system. The main objective of this study is to investigate the forming of plastic hinges, distribution of stresses, ductility and stiffness of these models. The results of current research showed good performance of composite systems including concrete column-steel beam in combination with steel shear wall and bracing system, are very desirable. The results show that the linear stiffness of models with X bracing and steel shear wall increase remarkably and their ultimate strength increase about three times rather than other RCS frames.

Keywords: concrete column; steel beam; connection; finite element; RCS; shear wall; bracing

1. Introduction

Composite Reinforced Concrete-Steel (RCS) frames including reinforced concrete columns and steel beams using the optimum combination of concrete and steel structural elements attracted a lot of attention in recent years. Advantages of composite structures rather to those of two other conventional ones are among performance characteristics under ultimate loads, economical conservation, and higher speed of construction.

Up to now RCS connections can be characterized as two main through-beam type and the through- column type categories in which beam through type behaved in a reliable manner under seismic loading than through- column type.

Lots of experimental studies have been conducted for studying the performance of RCS connections. Sheikh *et al.* (1989) tested interior RCS connections in 2/3 scale at University of

∗Corresponding author, Professor, E-mail: kheyroddin@semnan.ac.ir

http://www.techno-press.org/?journal=scs&subpage=6 ISSN: 1229-9367 (Print), 1598-6233 (Online)

Texas. Also RCS connections have been tested by Kanno (1993) at Cornell University. Kim and Noguchi (1998) studied the joint shear strength of RCS connections with different joint detailing through finite element analysis. An analytical analysis proposing of some suggestions to estimate the shear strength of interior and exterior RCS connections and an experimental program consisted of testing of 9 exterior RCS connections was carried out by Parra and Wight (2000, 2001) at the University of Michigan. Cheng and Chen (2005) tested Six RCS joints considering different parameters such as the joint stirrups, the effects of the cross-beam and the loading protocol. All researches, conducted on this type of composite structures until 2011 were reviewed by Li *et al*. (2011). Noguchi and Uchida (2004) investigated two RCS moment frames focusing on joint failure modes and the mechanisms through a nonlinear FEM analysis. Li *et al*. (2012) proposed a model and carried out a parametric study to investigate the behavior of composite concrete columns confined by continuous compound spiral ties and steel beams. Alizadeh *et al*. (2013) tested two new detailing interior RCS connections based on the Strong Column–Weak Beam (SCWB) criterion to study the performance of new detailing for RCS connections. Xu *et al*. (2016) present a new type of pre-pressed spring self-centering energy dissipation (PS-SCED) bracing system that combines friction mechanisms between the inner and outer tube members to provide the energy dissipation with the pre-pressed combination disc springs installed on both ends of the brace to provide the self-centering capability (Xu *et al*. 2016). Cao *et al*. (2014) studied the seismic performance of reinforced concrete (RC) frames strengthened by profiled steel sheet bracing which takes the influence of infill walls into consideration. A new structural bracing system named, Hat Knee Bracing (HKB) with a special form of diagonal braces, which is connected to the knee elements instead of beam-column joints, is investigated by Jafar Ramaji and Mofid (2012). Bazzaz et al. studied linear and nonlinear behavior of steel frames with off-centre bracing system and ductile element to get the best position of these bracing elements using finite element methods (Bazzaz *et al*. 2012). Some numerical studies have been performed using ANSYS software on a frame with off-centre bracing system with optimum eccentricity and circular element created. Furthermore, linear and nonlinear behavior of these steel frames with diagonal bracing system and the same circular element are compared in order to introduce a new way of optimum performance for these dissipating elements (Bazzaz *et al*. 2015).

2. Description of the test conducted by Chin-Tung Cheng, Cheng-Chih Chen

In this study, the seismic behavior of concrete column to steel beam connection in two modes, with and without slab was investigated in National Center for Research on Earthquake Engineering (NCREE), Taiwan (Fig. 1). Totally, six cross-shaped connections were created and evaluated. All the specimens in this test have identical dimensions for steel beams (H596×199×10 ×15) and concrete columns (65×65 cm). Based on existing load combinations, the dimension of beams for the highest roof to the first story were obtained H596×199×10×15, H366×199×7×11 and H500×200×10×16, respectively which in the all of these tests, the specimens were related to the first story. The concrete column is reinforced with 12 longitudinal rebars of number 11 (φ11) (Cheng and Chen 2005). Fig. 2 demonstrates cyclic displacement applied to the end of beams.

3. Finite element materials modeling of RCS composite connection

Concrete damaged plasticity model (CDPM) is used in all products of ABAQUS where the

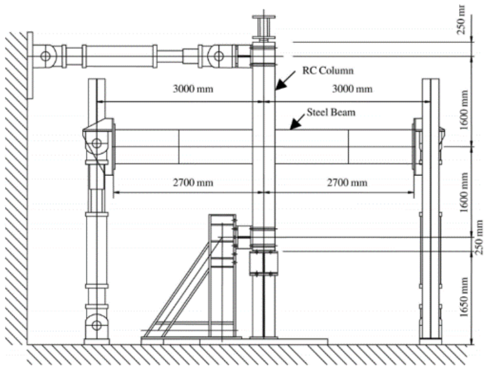

Fig. 1 Schematic test set up

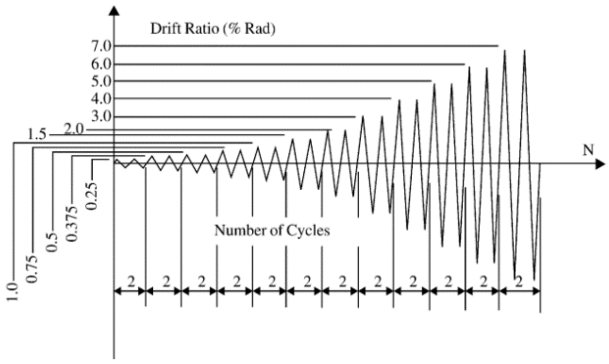

Fig. 2 Applied cyclic displacement to the end of beams

concrete is under various loading such as cyclic loads. The basis of this constitutive model is isotropic damage coefficient. In this study, this behavior characteristic is used for concrete material and the behavior described in Section 3.2 is used for steel material.

3.1 Concrete material

This diagram is determined based on uniaxial compressive test of concrete. For compressive concrete, three parts of the diagram will introduced (Fig. 3). The first part assumed to be elastic until the proportional limit stress. The value of this limit -stress assumed to be equal to $0.4f'_c$ in which f'_c is the compressive strength of concrete (ENV1992-1-1 1991). Strain ε_{c1} corresponds to stress 0.0022. The Young's modulus will be calculated on the basis of ENV 1992-1-1, Eurocode-2, and Poisson's ratio will also considered equal to 0.2. The second part of diagram which has a parabolic shape, starts from a point with limit stress and continues until it reaches the highest compressive strength of concrete, f'_c. This part of the diagram will be determined by the following equation 1

$$\sigma_c = \left(\frac{kn - n^2}{1 + (k-2)n}\right) f_{ck} \tag{1}$$

where

$$n = \frac{\varepsilon_c}{\varepsilon_{c1}} \tag{2}$$

And $\varepsilon_{c1} = 0.0022$, which the strain is maximum in compressive stress.

$$k = 1.1 E_{cm} \times \frac{\varepsilon_{c1}}{f_{ck}} \tag{3}$$

Where, E_{cm} is the modulus of elasticity of concrete.

The third part of stress-strain diagram is the descending part from f'_c to rf'_c in which reduction factor, r is assumed to be equal to 0.85. The final strain of concrete (ε_{cu}) is equal to 0.01 in the failure related to stress rf'_c. Fig. 4 also demonstrate tensile stress-strain curve for concrete used in

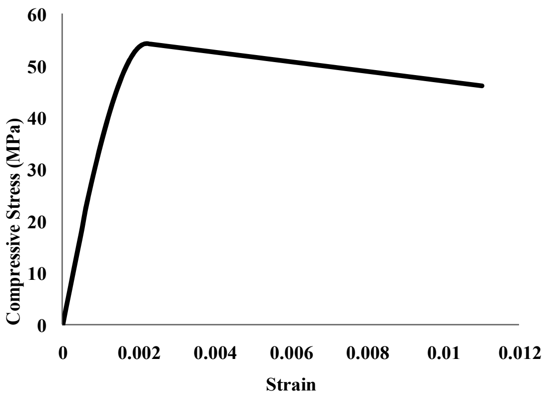

Fig. 3 Compressive stress-strain curve for concrete with compressive strength of f'_c = 54 MPa

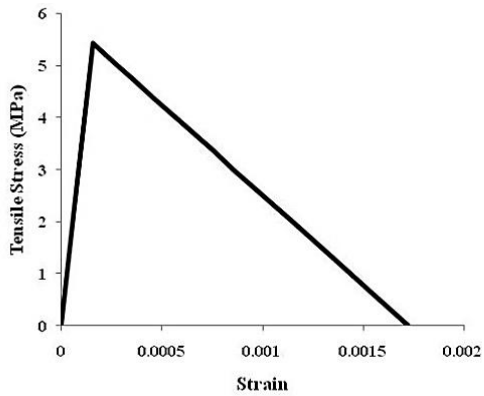

Fig. 4 Tensile stress-strain curve for concrete with compressive strength of f'_c = 54 MPa

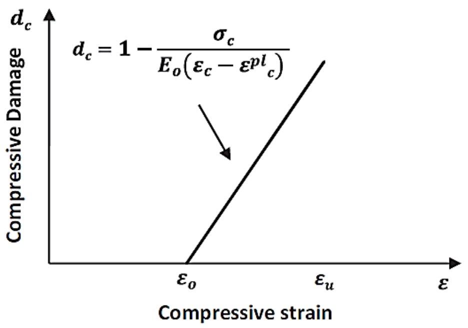

Fig. 5 Compressive damage curve

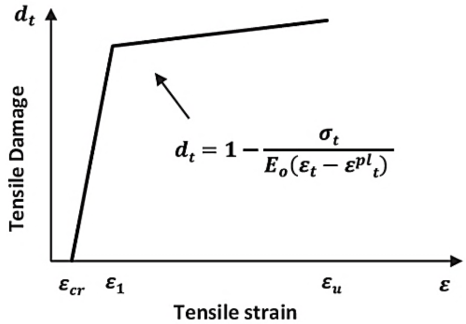

Fig. 6 Tensile damage curve

this study.

Damage was introduced in concrete damaged plasticity model in tension and compression according to Figs. 5-6, respectively. Concrete damage was assumed to occur in the softening range in both tension and compression. In compression the damage was introduced after reaching the peak load corresponding to the strain level, ε_0. The other concrete material parameters that were used in the presented analyses are: the modulus of elasticity E_0, the Poisson's ratio v and the compressive and tensile strengths of the selected slabs. The concrete damaged plasticity model considers a constant value for the Poisson's ratio, v, even for cracked concrete. Therefore, in the analyses presented herein, the value v = 0 was assumed. The dilation angle ψ was considered as 40°, the shape factor, K_c = 0.667, the stress ratio $\frac{\sigma_{b0}}{\sigma_{c0}} = 1.16$ and the eccentricity ε = 0.1 (Abaqus 2010).

3.2 Steel materials

Von-Misses constitutive models are used for modeling the behavior of steel in beams, longitudinal and transverse reinforcing bars, and other steel parts. The steel behavior is introduced in the software as Bilinear Elastic-Plastic curve.

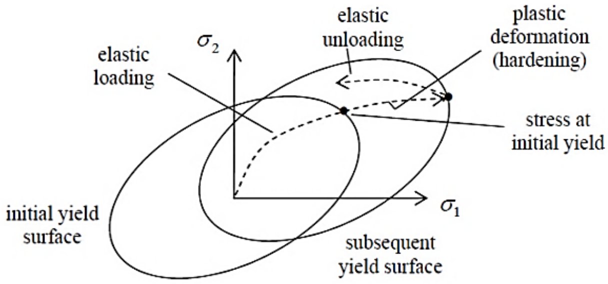

Fig. 7 Kinematic hardening; a shift by the back-stress

The hardening behavior rule of most materials appears to be a combination of the isotropic and kinematic type of hardening, sometimes accompanied by a change of shape of the yield surface. The isotropic model implies that, if the yield strength in tension and compression are initially the same, i.e., the yield surface is symmetric about the stress axes, they remain equal as the yield surface develops with plastic strain. In order to model the Bauschinger effect, and similar responses, where a hardening in tension will lead to a softening in a subsequent compression, one can use the kinematic hardening rule. This is where the yield surface remains the same shape and size but merely translates in stress space (Fig. 7).

The elastic-plastic behavior with the linear kinematic hardening was used as the material model.

4. Boundary condition

In the experimental tests, the concrete column belongs to the first story and its connection to the foundation is fixed. Therefore, in the software modeling, all the translational and rotational degree of freedom (DOF) U_1, U_2, U_3, UR_1, UR_2, UR_3 at the column toe attached to a rigid support plane, is fixed. Actually, this boundary condition is applied to the reference point of rigid plane, and the movement of other nodes is affected by it. In the performed experimental test a hydraulic actuator, keeps the column in its current state before testing begins, and let it to rotate just in plane. For simulating the boundary condition in the top of the column, only UR_2 allowed to be free. The beams are also allowed to have displacement at their two ends in up and down directions, meaning

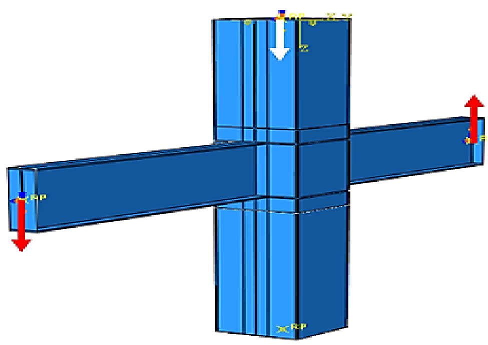

Fig. 8 Applied displacement to the ends of beams and the axial load exerted on the top of column in FE model

Table 1 Determining the mesh size (Sensitivity analysis)

Mesh factors	0.8	1	1.5	2	2.25	2.5	3	3.5
Element size (mm)	28	35	52.5	70	78.75	87.5	105	122.5

that they can rotate only in plane. In the finite element model at the two ends of beams only DOFs U_3 and UR_2 were allowed to be free and the rest of other DOFs including U_1, U_2, UR_1 and UR_3 were closed (Fig. 8).

5. Type and size of elements

The concrete column was modeled by three-dimensional elements (C3D8R) available in ABAQUS software library that are 8 node elements and are used for nonlinear analysis including the impact of two materials, large deformations, plasticity, and failures. The steel beams and other connected parts are also discretized into elements. Reinforcing bars and rigid support planes also have been modeled by elements T3D2 and R3D4, respectively. In order to reduce the time analysis, coarse elements are used in many parts and fine elements are used in the areas of connection zone. The dimension of elements in most parts of beams and columns is 35 mm, while the minimum size of them is 18 mm.

In this study, the size of the elements of the beam and the column was changed as shown in Table 1. The analysis was continued until the time when, with a change in element size, the difference between the finite element diagram and the experimental diagram was negligible.

Finally, given the above discussions, through a mesh size sensitivity analysis, 35 mm was selected for the beam and the column; it is the factor of 1 in Table 1. As can be seen in Fig. 9, when the dimensions of the elements reach these values, the difference between the diagrams is negligible.

6. Investigation the results of finite element analysis and experimental results of specimen INUC

As it can be seen in Fig. 10, the results of numerical analyses and experimental tests are

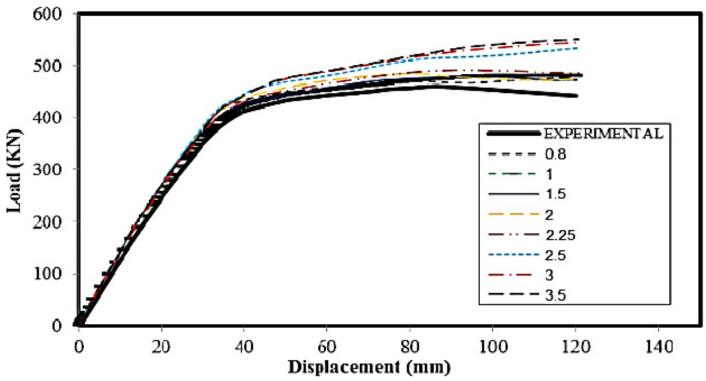

Fig. 9 The load-displacement curve in mesh sensitivity analysis

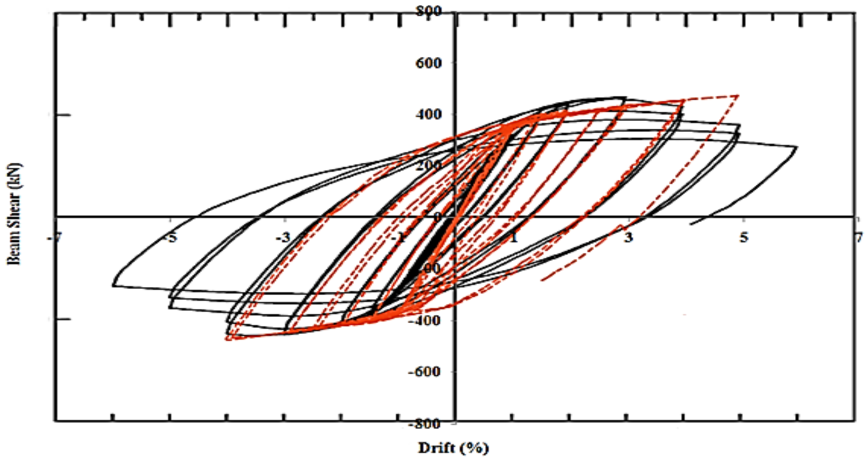

Fig. 10 Beam shear versus displacement of the end of beam; comparison between FE and experimental model

coincident together in low drifts to less than 4%. They have quite similar and stable behaviors. For a drift equals to 4% both results experienced their maximum strength. However, for greater drifts because of the elastic-plastic behavior of used finite element constitutive model for steel in which failure is not defined in it, the strength is not reduced and for drift equals up to 7%, the strength is almost constant, while in the experimental model, the strength has reduced in higher cycles after it reached its maximum strength in drift 4%.

According to Figs. 11-12, the column sustains little damage. Further, diagonal cracks occur only at the connection zone in the concrete column, and transverse cracks occur only at the areas immediately above and below the steel beam.

The test results show that all specimens performed in a ductile manner with plastic hinges formed at the beam ends near the column face, where local buckling took place successively at the beam flange and web, and only minor damage such as cracks was observed in the column and the panel zone.

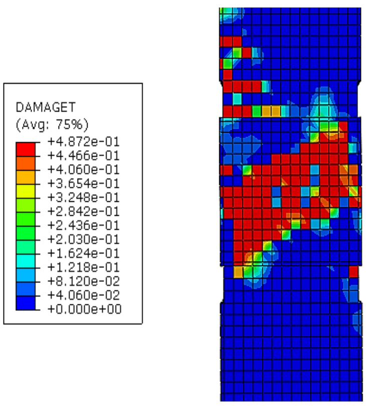

Fig. 11 Concrete cracking pattern in finite element analysis

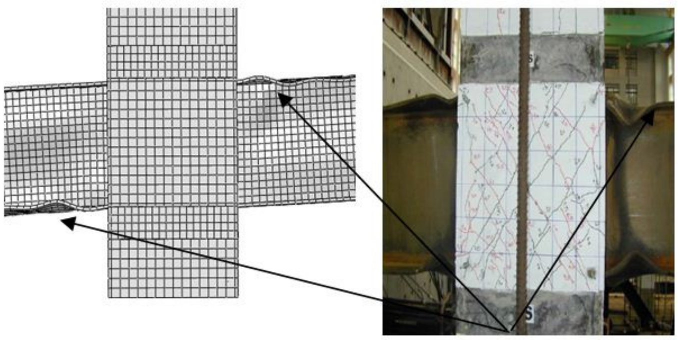

Fig. 12 Local buckling at the beam flanges in experimental model (Cheng and Chen 2005) and finite element model

7. Parametric study

In this part, in order to investigate the behavior of reinforced composite RCS connections, nonlinear static analysis is conducted, and comparison has been performed between following five RCS frame specimens:

- Specimen 1: composite RCS frame with concrete column and steel beam
- Specimen 2: composite RCS frame with concrete column and steel reduced beam section (RBS).
- Specimen 3: composite RCS frame with X bracing gusset plates
- Specimen 4: composite RCS frame with steel concentric X bracing
- Specimen 5: composite RCS frame with steel shear wall

7.1 Specimen 1

This frame includes a composite RCS connection of monolith beam type analyzed under Pushover loading. For this purpose, a displacement will be applied to upper joints of the frame. This specimen includes concrete columns with the dimension of 1730×400×400 mm which are reinforced with 16 longitudinal rebars of ϕ18. Φ10 rebar is also used as the stirrup in columns and connection area. Table 2 illustrates the specimen material properties used in the parametric study.

The used steel beam section in this specimen is IPE 300 with 2800 mm of length. *L* shape stirrups are used that are crossing through the holes created in the beam web. In the area of panel zone, palates of size 430×260×8 mm are welded to the bam web to reinforce it. This specimen includes steel straps around the column at the top and bottom of the beam (Band Plate) which their height and thickness are 80 mm and 15 mm, respectively. Moreover this specimen contains face bearing plate with a width equal to beam flange width, and a length equal to beam web height and 15 mm of thickness. Fig. 13 shows a general illustration of specimen details, FEM model and its constitutive components. As can be seen in this figure, as regards to the symmetrical shape of tested specimens, only a half of the frame is modeled in order to reducing the calculation volume. All units are considered by newton and millimeter. In this model, the connection of the column toe is pinned type, accordingly it will be modeled conical in the software in order to simulating pinned connection. The beam parts, double plate to reduces shear stress and prevent the formation of plastic hinge in the connection zone (AISC 360-10 2010), FBP plate, Band plate, and the support of concrete column are modeled using three-dimensional solid element. For modeling longitudinal reinforcing bars and stirrups, two dimensional truss elements named wire is used.

Compressive strength, tensile strength, modulus of elasticity, and Poisson ratio of the concrete material are considered equal to 50 MPa, 4 MPa, 33541 MPa, and 0.2, respectively.

Table 2 Specimen material properties

Steel beam	Beam flange	F_y = 356.6 MPa	F_u = 493.4 MPa
	Beam web	F_y = 368.8 MPa	F_u = 496.3 MPa
Longitudinal rebar, ϕ18		F_y = 523 MPa	F_u = 669 MPa
Transverse rebar, ϕ10		F_y = 408 MPa	F_u = 615 MPa
Strength of concrete		f'_c = 50 MPa	

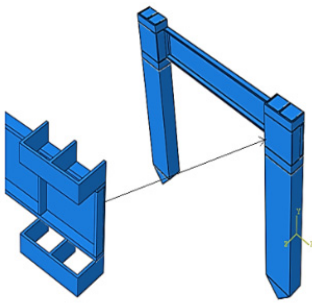

Fig. 13 Connection details in composite RCS frame

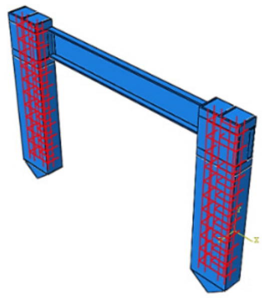

Fig. 14 Placing the longitudinal and transversal rebars

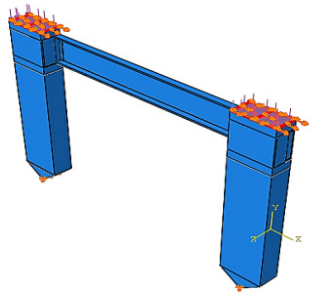

Fig. 15 Applying load on the column

Considering nonlinear geometric and material effects, nonlinear elastic analysis (static general), is used for analyzing the model. The model analysis has performed in two steps, so that in the first step, the gravity load is applied on the columns, then lateral displacement is applied to the column head.

The interaction between concrete and steel parts in the connection area has defined by tangential elements (tangential behavior) and penalty method with a friction coefficient of 0.3. In order to define concrete and steel parts to be not penetrating in each other, normal tangential elements with hard contact are used in the connection area. All the contact properties illustrated above are defined for software by general contact. By defining this contact element, the software assigns the defined properties to all the concrete and steel surfaces in contact with each other.

As can be observed in Fig. 14, in order to consider the interaction between reinforcement bars with concrete, embedded region is used. For assigning boundary condition and loading to model, gravity load is applied to the top of columns, and lateral displacement is also applied to it at both sides (Fig. 15).

In all the specimens, three-dimensional 8-nodes solid elements (C3D8R) are used for meshing steel beam, concrete column, and steel parts and for meshing longitudinal and transversal bars, and steel panels, 2-node truss elements wire (T3D2) and 4-node shell elements (S4R) have been used.

7.2 Specimen 2

In the modeling of RCS frame with concrete column and reduced beam section (RBS), all the geometry and material properties of the model are similar to the specimen 1, with the exception that in this specimen, reduced section is used for beam flange as it can be seen in Fig. 16.

7.3 Specimen 3

In this model, the bracing gusset plates in the four corners of the frame (Gusset Plate), with dimension of 200×200×10 mm, and 200×200×7.5 mm are connected to the composite RCS frame. The interfaces between gusset plates, beams and columns are tied together. The gusset plates also should be fully consistent with the axis of the beam and column. In the definition of boundary condition, displacement of the gusset plates is closed in bottom of the frame. Other geometric and material properties and loading condition are similar to specimen 1 (Fig. 17).

7.4 Specimen 4

In addition to all the specifications defined in the specimen 3, an X bracing with bracing gusset plates will be added. The dimension of gusset plate is 400×200×7.5 mm, and the brace section is U-shaped channel (60×30×6 mm) with a length of 2120 mm. The selected section area of the brace, is a used section for other similar research with beam and column which after investigating about the accuracy of this selection, it is used in this study (Fig. 18).

7.5 Specimen 5

In the modeling of composite RCS frame with concrete column and steel beam with steel shear wall, all the geometric and material properties are similar to the specimen 1, with this exception that in this specimen, plates connecting the shear wall to columns are of dimension 1350×200×5 mm that is used as connector plate between steel panel and concrete column and is modeled using three-dimensional solid element. In the steel panel, at the place where the panel thickness (2 mm) is very small than other two dimension, and stresses are negligible in the direction of model

Table 3 Yielding and ultimate strength of steel in specimen 5

Steel member	Yielding stress (MPa)	Ultimate stress (MPa)
Plates connecting steel panel to column	240	370
Steel panel	190	280

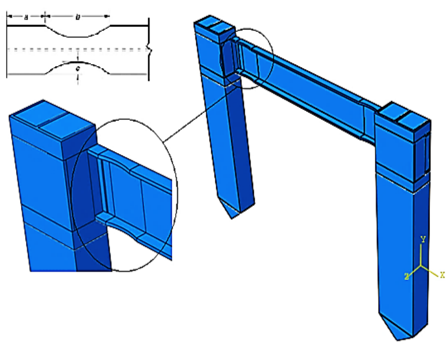

Fig. 16 RBS beam and RCS frame connection

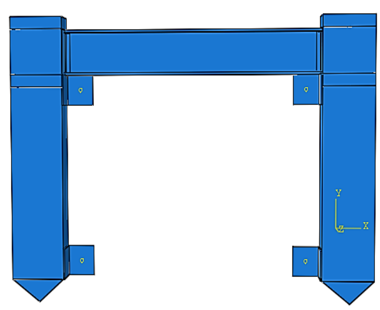

Fig. 17 RCS frame with X-bracing gusset plates

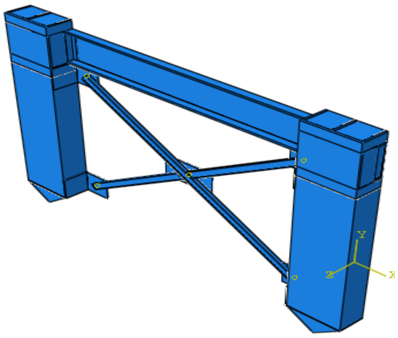

Fig. 18 RCS frame model with X bracing

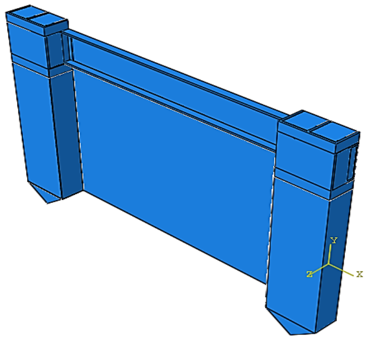

Fig. 19 RCS frame model with steel shear wall

thickness, shell elements are used in the modeling. In the shell elements, it will be assumed that plane sections perpendicular to the sell plane, remains as a plane (Fig. 19).

Given that in the steel shear walls under impact caused by transport or even welding in plate, a pre-primary buckling occurs in steel panel in most cases. Therefore, in order to consider this occurrence in the software, an initial geometric imperfection in the form of a displacement equals to 2 mm perpendicular to the panel plane have been applied before applying the lateral load. This pre-primary buckling influences parameters such as stiffness and strength. The yielding and ultimate strength of wall components are presented in Table 3.

8. Study cracking results, stress distribution, stiffness, strength and ductility of the specimens

In this part, the most important parameters in monotonic loading response are comparing. In technical literature, general design criteria for capability and performance of structural systems are strength, stiffness and ductility. So cracking patterns, stress distribution, stiffness, strength and ductility of the systems in modeled frames are investigated.

8.1 Cracking and failure stages of the models

In specimen 1, the composite RCS moment frame is a force resistant system, thus forces lead to creating flexural cracks in the concrete column. When loading starts, and by increasing loading steps, the cracks occur from connection area, and at the bottom of connection area. As the loading steps will continue to the number and depth of the cracks increase. In the moment frame, first crack was observed in 84.148 kN of load, and 9.45 mm of displacement that is a soft crack at the bottom of beam on the column. Cracks will continue with an increase in load values, hence, it can be said that in this model, collapsing in the structure occurs with creating plastic joint in the upper half of column beneath the beam connection (Fig. 20).

In specimen 2, which reduced beam section is used, the cracking process is almost similar to the specimen 1 with a slight difference. Although according to Fig. 21, the amount of damage is less than specimen 1, and the corresponding load and displacement to the first cracking in the column, are 82.58 kN and 9.28 mm, respectively that is less than specimen 1.

In specimens 3, and 4 according to Figs. 22-23, because of the brace and the stress concentra-

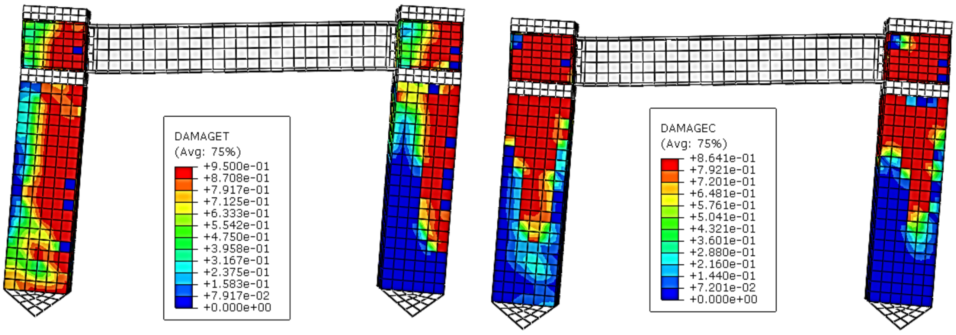

Fig. 20 Compressive and tensile concrete damage in the frame of specimen 1

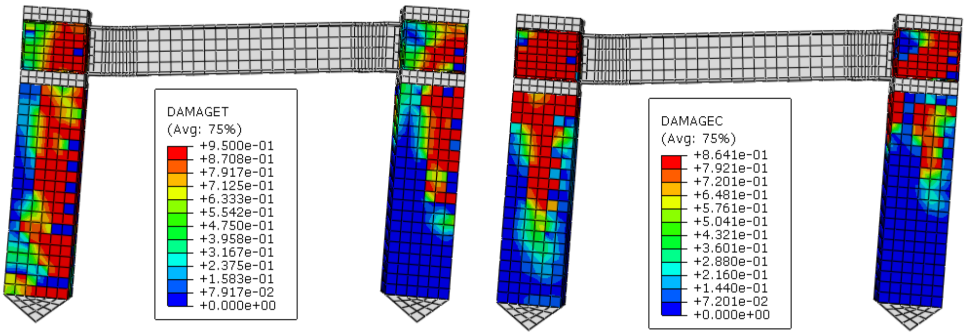

Fig. 21 Compressive and tensile concrete damage in the frame of specimen 2

tion in the connection of brace to the column, first shear cracks starts from the column toe and then crosses from the corner at bottom of the connection into the connection. First cracks in the composite frame are because of the way of transferring load to braces which are few and shallow. First cracks in the specimen 3 occur in load 131.28 kN, and displacement 5.75 mm, and in specimen 4, it occurs in load 316.65 kN and displacement 4.87 mm. This indicates the bracing system has the required load for creating first crack.

Until the braces were in the bearing system, and buckling didn't occurred, the cracks slowly developed in number and depth with loading steps. Although, when buckling occurs in the braces, the crack propagation speeds up. Existence of steel sheath in the connection, and the further cracks in column compared to the connection, leads to develop cracks in the longitudinal direction of the column. In these two models, collapsing occurs with creating plastic joints in the area of column toe.

In specimen 5, according to Fig. 24, concrete failure starts from the bottom of column adjacent to gusset plates of steel panel, and develops in longitudinal direction of gusset plates on the column. As can be observed, in this model, tensile cracks developed slightly in the connection. First cracks in this specimen, occur under load 535.23 kN and displacement 9.1 mm.

8.2 Stress distribution

In the RCS single frame, stresses increase in the longitudinal rebar of column close to the connection area with an increase in the applied load. Actually, first and second plastic joint occurs

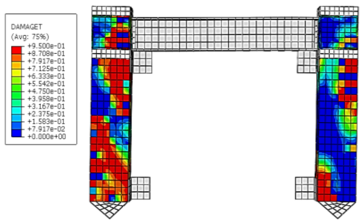

Fig. 22 Tensile concrete damage (specimen 3)

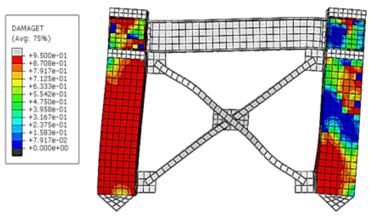

Fig. 23 Tensile concrete damage (specimen 4)

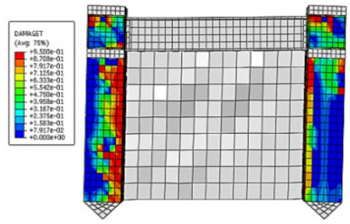

Fig. 24 Tensile concrete damage (specimen 5)

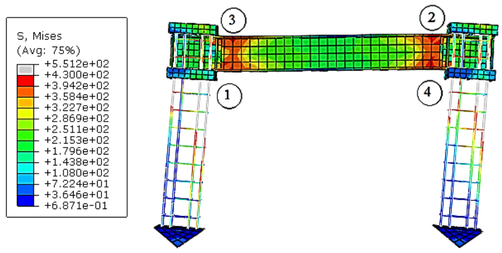

Fig. 25 Von-Mises stress contours of steel unreduced beam section

in the longitudinal reinforcing bars of column, immediately after that in bottom-right flange of beam under a load of 154.63 kN and displacement of 21.44 mm (Fig. 25). With continuing of loading, a greater area of beam flange and beam web, next to the column and also longitudinal and transversal rebar will attain the yielding stress. Thereafter, the frame enters plastic response. Finally, the structure collapses with yielding of longitudinal bars of the column, and creating the fourth plastic joint in the plastic area in load 190.53 kN and displacement 38.86 mm, and will be unstable.

In the specimen 2, the process of stress distribution is similar to specime1 (Fig. 26). However, the first plastic joint occurs on reduced beam section in both sides under load 125.45 kN and displacement 16.59 mm. With continuing the loading, plastic joints will be created perfectly in the area of recused section on the beam. Thereafter, longitudinal bars at the bottom of left column yields and then the frame enters plastic region. Finally, the structure will collapse due to the creation of fourth plastic joint under load 177.66 kN and displacement 51.9 mm.

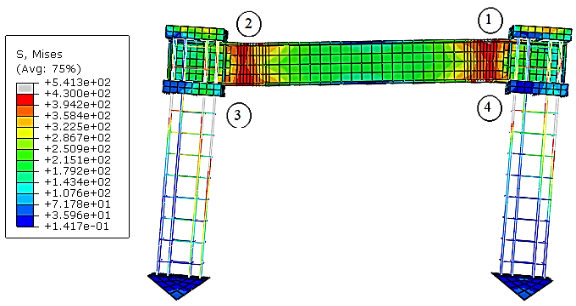

Fig. 26 Von-Misses stress contours of steel reduced beam section

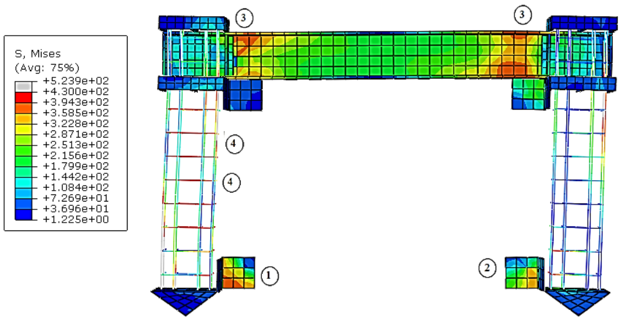

Fig. 27 Von-Misses stress contours of steel beam in composite frame with bracing gusset plates

As can be seen in Fig. 20, plastic joint is occurred in a greater area of the beam flange and its web in steel reduced beam section. This will increase ductility and energy absorption in the frames with reduced beam section compared to unreduced beam section.

In specimens 3 and 4, according to Figs. 27-28, first the bottom plates of bracing connection and then the area on the beam next to the connection are wielded. Because of the ability to absorb and withstand lateral force, braces reduce the speed of stress distribution in the frame as long as they are in the system. In the case of moment frame, with regards to the fact that energy absorption will occur in the connections which are of the most important parts of moment frames, the stress develops in it, more quickly. Until the brace is not removed from the system, the stress in bracing system and gusset plates is more than the frame. The load will be carried by the frame and stress will increase quickly when the brace buckles.

According to Fig. 27, in the specimen 3 which frame and gusset plates are exist, the first plastic joint occurs on the brace gusset plate at the bottom under load 205.83 kN, and displacement 11.9 mm. Thereafter, plastic joint is created in right brace gusset plate and over the beam flange. Then, longitudinal and transversal bars of the column start to yielding, concurrently. As expected, the strength of this frame is more than the RCS single frame. Finally the structure failed and will be unstable, in which in the plastic area the applied load and displacement are 287.1 kN and 31.67 mm, respectively.

In specimen 4, in which the stress increasing in the braces is more than stress increasing in the moment frame, according to Fig. 28, the first plastic joint occurs in the brace under load 342 kN, and displacement 5.203 mm. Continuing the loading, plastic joint will be created along the second brace and in the bottom brace gusset plate. First, the braces are completely yielded under load

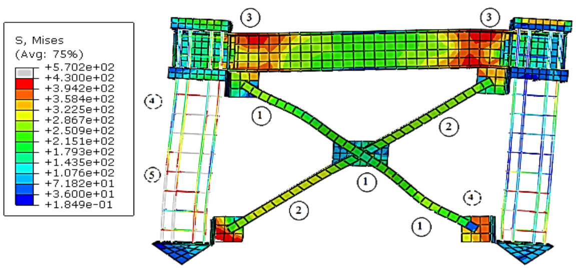

Fig. 28 Von-Misses stress contours of steel beam in composite frame with X bracing

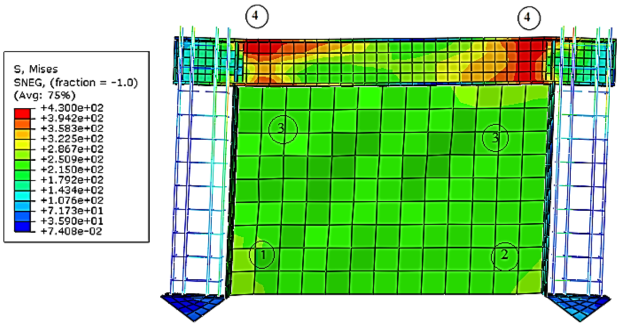

Fig. 29 Von-Misses stress contours of steel beam in composite frame with steel shear wall

445.67 kN and begins buckling. After the braces have been yielded, the third plastic joint will be created with yielding of beam flanges and the structure response enters plastic region. Finally, the structure fails after crating the next plastic joints on longitudinal bars of column beneath the connection and at the column toe under load 518.75 kN, and displacement 32.09 mm.

In this model, with a little difference with model 3, the longitudinal reinforcing bars of the column reach the yield point later. The bracing failure and their removing from the bearing system of structure, will occur under compressive buckling.

In the specimen 5, first, plastic joint occurs at the bottom corner of steel panel near the column under load 334.35 kN and displacement 1.76 mm. Thereafter, the yielding draws up into the middle and upper parts of the panel with increasing the load. After the entire yielding of steel panel under load 590.92 kN, the moment frame has taken the structure bearing role, and next plastic joint will be created in the beam flange next to the column. Finally, the structure failure in the plastic region occurs under load 692 kN (Fig. 29).

8.3 Investigation the initial stiffness of models

In this part, the contribution of stiffness of each frame components in the above-mentioned five specimens will be calculated. Method for calculating the stiffness of each section separately is so that first, the total stiffness of all four specimens will be calculated, afterward by deduction the stiffness of composite RCS single frame from obtained results, the contribution of each part will be calculated.

According to Fig. 30 and the obtained results in Table 4, it can be observed that the existing of bracing gusset plates in the four corners of frame, X bracing with gusset plates, and shear wall in the composite RCS frame lead to increasing the initial stiffness in the composite RCS single frame equal to 3.3, 5.54 and 17.76 times, respectively that are significant values. Moreover, according to Table 5, the contribution of gusset plates in the stiffness of composite RCS frame with gusset plates is 69%, the contribution of only X bracing is 56%, and the contribution of shear wall in the frame stiffness equals to 94%.

Moreover, by comparing the specimens, it can be resulted that the contribution of single frame, bracing gusset plates, and the brace itself in composite braced frame (specimen 3) is about 13.2%, 30.5%, and 56.3%, respectively. The results indicate that X bracing in the composite RCS frame can increase the initial stiffness of frame up to 2 times. From the other side, the stiffness of composite frame with shear wall is about 2.35 times more than composite frame with X bracing which it may be because of using the entire capacity of used steel in the shear wall system and the buckling of compressive brace.

8.4 Bearing strength

By investigating the load-displacement curve of models, it can obviously be seen that the bracing, bracing gusset plates and the shear wall have increased the bearing capacity.

At the first, load-displacement curve for two specimens 1 and 2 are compared. As can be seen

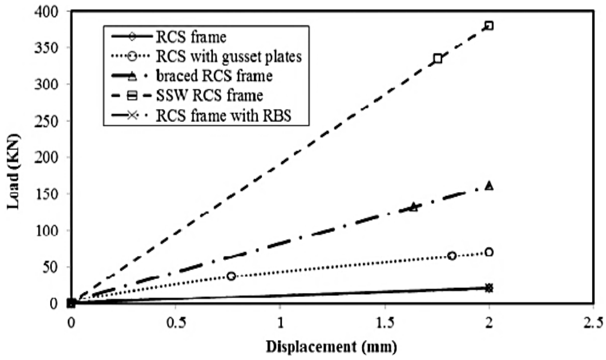

Fig. 30 Diagram of initial stiffness of frames

Table 4 The comparison of stiffness of five composite frame specimens compared to single frame in finite element

Specimens	Composite RCS frame	RBS beam	Gusset plates	Bracing	Shear wall
Specimen stiffness (kN/mm)	10.695	10.695	35.3	80.64	190
Stiffness factor	1	1	3.3	7.54	17.6

Table 5 The contribution of gusset plates, X bracing, and shear wall in the initial stiffness of frames

Member	Gusset plates	Single bracing	Steel shear wall
Contribution percent	69%	56.3%	94%

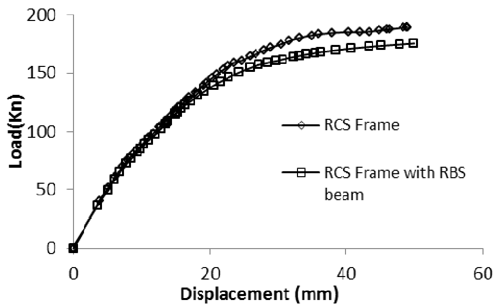

Fig. 31 Comparison of load-displacement curves for specimens 1 and 2

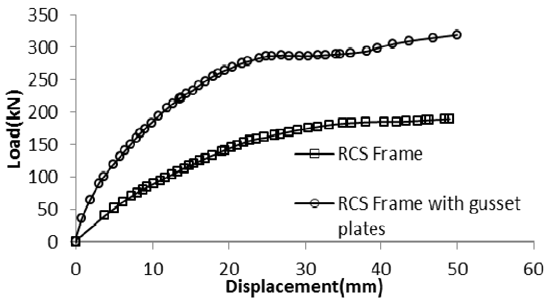

Fig. 32 Comparison of load-displacement curves for specimens 1 and 3

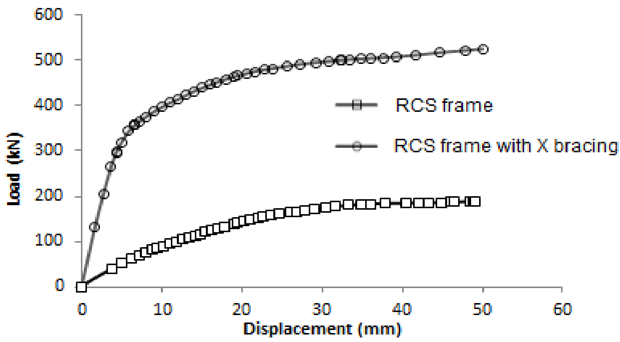

Fig. 33 Comparison of load-displacement curves for specimens 1 and 4

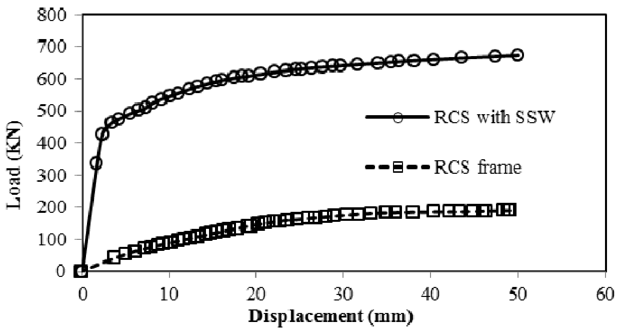

Fig. 34 Comparison of load-displacement curves for specimens 1 and 5

in Fig. 31, the composite RCS moment frame has an ultimate strength equal to 190 kN while in the specimen 2 with reduced beam section, the value of ultimate strength is 175.5 kN. These values indicate that if reduced beam section used, the bearing capacity of frame decreases about 8%.

In order to comparison models 1 and 3, by referring to Fig. 32, can be observed that the value of ultimate strength of frame with bracing gusset plates has obtained equal to 319.336 kN. This comparison indicates that the bearing capacity has been increased about 1.68 times.

In the Fig. 33, load-displacement curves of composite RCS frame and frame with X bracing are shown. The bearing capacity of the frame is equal to 525.16 kN that has increased significantly about 2.76 times compared to the single frame. In the model 5 that the composite RCS frame is

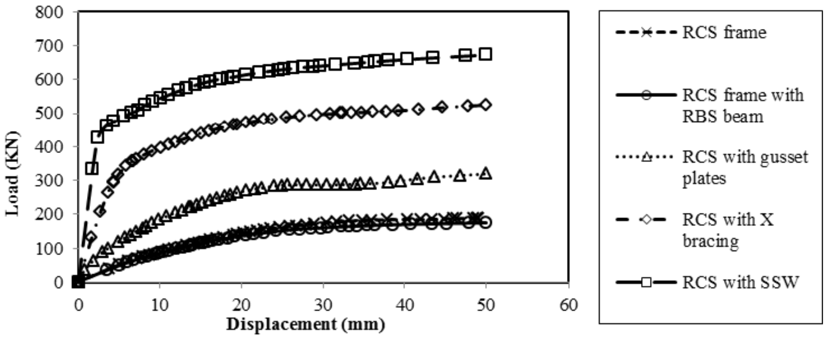

Fig. 35 Comparison of load-displacement curves for all the five specimens

reinforced with shear wall, the ultimate bearing capacity of the frame obtained equals to 672.64 kN that has increased about 3.54 times compared to single frame (Fig. 34). Furthermore, the bearing capacity of this system has increased about 28% compared to the bracing system.

Actually, the steel panel existing has led to increasing the yielding and ultimate load, this somehow indicates this system to act stiffer than concentric bracing. This topic has been studied more detailed in previous part related to stiffness.

The most ideal mode of wall behavior occurs when the plate (steel sheet) reaches yielding limit. However, in practice the steel plate buckles due to plate slenderness. Load-displacement curves of the analyzed five frames are compared in the diagram of Fig. 35.

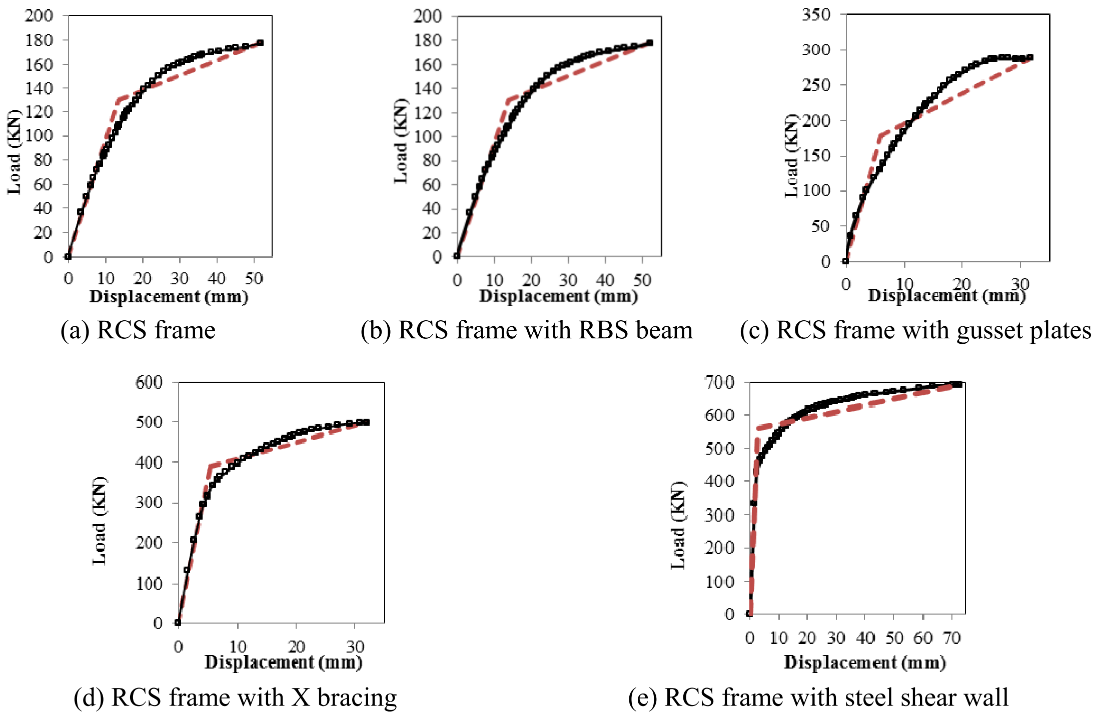

Fig. 36 Load-displacement curve (line in black) and idealized bilinear curve (line in red) of specimens

Table 6 Ductility factor of specimens

Frame	μ	Δ_y	Δ_{max}
1	2.98	13.05	38.86
2	3.78	13.73	51.8
3	5.33	5.942	31.67
4	6.32	5.359	32.09
5	24.85	2.93	72.81

8.5 Ductility

Fig. 36 shows load-displacement curves for analyzed specimens with the idealized bilinear curves. Ductility (μ) is equals to the ratio of final displacement (Δ_{max}) to displacement corresponding to yielding point (Δ_y) in the elastic-perfectly plastic curve. The amounts of frames ductility are compared together in table 6. The ductile response of steel structures occurs when steel reaches yielding. By contrast, their non-ductile response is a result of failure or instability. Therefore, the key parameter in designing ductile structures with maximum yielding in the elements of steel frames is to delay the beginning of instability and failure. To achieve this, the first step is to select the points for the yielding of steel in the frames. These points are called plastic hinges. With an increase in local buckling, the end of the beam flange undergoes failure. Therefore, the criterion for obtaining Δ_{max} in the specimens is the failure of steel at the points mentioned, such that, when the load is applied, the stress exerted on the steel at that point reaches the ultimate value entered in the software, and the steel undergoes failure. At this time, Δ_{max} resulting from loading the structure can be obtained from the software (FEMA-356 2000).

As it can be seen in Table 6, the ductility increases when the RBS beam is used. The ductility in model 3, that gusset plates are used in it, has become about 1.78 times, in model 4 that the frame is reinforced with bracing system, about 2.12 times, and in model 5 which steel shear wall is used in it, about 8.34 times.

9. Conclusions

The aim of this research is to evaluate the RCS composite frames in combination with RBS beam, braced plates, cross brace and steel shear wall in order to compare and investigate cracking pattern, stress distribution, improvement of plasticity, strength, and stiffness.

The advantage of steel braces is to speed up implementation, lack of construction complexity due to different braces type, easy and logical calculations and cost saving in comparison with existing methods. On the other hand, steel shear walls are also very simple in terms of implementation and there is no particular complexity in them.

Five analytical samples have been modeled, analyzed, and compared in this research. More plasticity and energy absorption can be seen in the frame with reduced beam section than frame with unreduced flange section.

9.1 Stress distribution

Adding a brace to RCS composite frame changes failure mechanism, and causes column longitudinal reinforcement reach later to the yield point. Braces also reduce stress distribution speed in the frame because of the ability to absorb and bear lateral force until they are in the system.

9.2 Forming plastic hinges

In model 5 (steel shear wall has been used), the entire steel panel reaches its yield point at the first, and then plastic hinge is formed in the beam flange and web to be a desirable mechanism. In fact, the presence of steel panel leads to an increase in the final yielding load of the structure to a considerable extent.

9.3 Bearing capacity

The use of steel brace and steel shear wall increase the bearing capacity of the system. On the other hand, capacity in the shear wall system has been significantly increased compared to bracing system.

9.4 Stiffness

Stiffness of shear wall system is higher than X bracing system. So that the initial stiffness of steel shear wall system is about 2.3 times of the initial stiffness of bracing system. Also the behavior of shear wall system in the plastic region and the amount of energy absorption is more suitable than bracing systems.

In addition to high shear resistance and stiffness of steel shear walls, this system in terms of the extent of sheet connection with the frame around (lack of a centralized connection such as bracing system) and the gradual formation and uniform tension in steel sheet, and good ability to adjust the tensions until reaching the final load is more reliable than other conventional systems and its energy absorption is gradual and with minimal local and general weakness. Also the force corresponding to the first crackup in the frame is increased by suitable reinforcement of frame.

References

Abaqus (2010), Abaqus analysis user's manual, Version 6.10, Dassault Systems.

AISC 360-10 (2010), Specification for Structural Steel Buildings, Chicago, IL USA.

Alizadeh, S., Attari, N.K.A. and Kazemi, M.T. (2013), "The seismic performance of new detailing for RCS connections", *J. Construct. Steel Res.*, **91**, 76-88

Bazzaz, M., Kheyroddin, A., Kafi, M.A. and Andalib, Z. (2012), "Evaluation of the seismic performance of off-centre bracing system with ductile element in steel frames", *Steel Compos. Struct.*, *Int. J.*, **12**(5), 445-464.

Bazzaz, M., Andalib, Z., Kheyroddin, A. and Kafi, M.A. (2015), "Numerical comparison of the seismic performance of steel rings in off-centre bracing system and diagonal bracing system", *Steel Compos. Struct.*, *Int. J.*, **19**(4), 917-937.

Cao, P., Feng, N. and Wu, K. (2014), "Experimental study on in-filled frames strengthened by profiled steel sheet bracing", *Steel Compos. Struct.*, *Int. J.*, **17**(6), 777-790.

Cheng, C.T. and Chen, C.C. (2005), "Seismic behavior of steel beam and reinforced concrete column connections", *J. Construct. Steel Res.*, **61**(5), 587-606.

ENV1992-1-1 (1991), Eurocode-2: Design of concrete structures, Part 1: General rules and rules for building, Brussels, Belgium.

FEMA-356 (2000), Prestandard and Commentary for the Seismic Rehabilitation of Buildings, Washington.
Jafar Ramaji, I. and Mofid, M. (2012), "On the characteristics and seismic study of Hat Knee Bracing system, in steel structures", *Steel Compos. Struct., Int. J.*, **13**(1), 1-13.
Kanno, R. (1993), "Strength, deformation, and seismic resistance of joints between steel beams and reinforced concrete columns", Ph.D. Dissertation; Cornell University, Ithaca, NY, USA.
Kim, K. and Noguchi, H. (1998), "A study on the ultimate shear strength of connections with RC columns and steel beams", *J. Struct. Construct. Eng.*, **507**, 163-169.
Li, W., Li, Q.N., Jiang, L. and Jiang, W.S. (2011), "Seismic performance of composite reinforced concrete and steel moment frame structures—state-of-the-art", *Compos. Part B: Eng.*, **42**(2), 190-206.
Li, W., Li, Q.N. and Jiang, W.S. (2012), "Parameter study on composite frames consisting of steel beams and reinforced concrete columns", *J. Construct. Steel Res.*, **77**, 145-162.
Noguchi, H. and Uchida, K. (2004), "Finite element method analysis of hybrid structural frames with reinforced concrete columns and steel beams", *J. Struct. Eng.*, **130**(2), 328-335.
Parra-Montesinos, G. and Wight, J.K. (2000), "Seismic response of exterior RC column-to-steel beam connections", *J. Struct. Eng.*, **126**(10), 1113-1121.
Parra-Montesinos, G. and Wight, J.K. (2001), "Modeling shear behavior of hybrid RCS beam–column connections", *J. Struct. Eng.*, **127**(1), 3-11.
Parra-Montesinos, G. and Wight, J.K. (2003), "Towards deformation-based capacity design of RCS beam–column connections", *Eng. Struct.*, **25**(5), 681-690.
Sheikh, T.M., Deierlein, G.G., Yura, J.A. and Jirsa, J.O. (1989), "Beam–column moment connections for composite frames: part 1", *J. Struct. Eng.*, **115**(11), 2858-2876.
Xu, L., Fan, X., Lu, D. and Li, Zh. (2016), "Hysteretic behavior studies of self-centering energy dissipation Bracing system", *Steel Compos. Struct., Int. J.*, **20**(6), 1205-1219.

CC